Domain wall duplication in a hard-soft spin-valve structure using the CoFe/Ir/CoFe artificial antiferromagnetic subsystem

S. Colis and A. Dinia*
IPCMS-GEMME (UMR 7504 du CNRS), ULP-ECPM, 23 rue du Loess, F-67037 Strasbourg Cedex, France
(Received 30 May 2002; published 15 November 2002)

We used magnetoresistance measurements to evidence a domain wall duplication between the soft and the hard layer in a hard-soft spin-valve-type structure. The spin valves are grown by molecular-beam epitaxy on MgO(001) substrates. For the sample composed only of the magnetically soft Fe/Co subsystem, the magnetization loop is square with a coercive field of about 25 Oe. After the growth of the 3-nm Cu decoupling layer and of the CoFe/Ir/CoFe antiferromagnetically coupled sandwich (hard layer) on the top of the soft subsystem, the magnetization minor loop of the soft electrode is shifted towards positive applied fields. Such a shift of the order of 5 Oe is attributed to an exchange-type interaction between the artificial antiferromagnetic sandwich (AAF) and the soft Fe/Co bilayer. As a consequence the domain wall structure of the AAF is duplicated into the Fe/Co soft electrode, despite the large (3-nm) layer thickness of the decoupling layer. This is further confirmed by magnetoresistance measurements, and supported by magnetic force microscopy observations and demagnetization studies.

DOI: 10.1103/PhysRevB.66.174425 PACS number(s): 75.60.Ch, 75.70.−i, 75.70.Pa

I. INTRODUCTION

Since the discovery of spin-valve systems[1] composed by a soft and a hard magnetic layer separated by a nonmagnetic spacer, this research area is the subject of intense developments. This is due to the fundamental interest of these systems as well as to their potential applications, such as high-density recording media or magnetic sensors. Two alternatives are widely used to ensure the rigidity of the hard layer. The first is the exchange-biased system in which an antiferromagnetic layer [FeMn,[2] NiO,[3] or IrMn (Ref. 4)] ensures the rigidity of the biased magnetic layer via exchange anisotropy. The second is the so-called artificial antiferromagnetic subsystem (AAF) for which the hard layer is composed of two ferromagnetic layers coupled antiferromagnetically through a nonmagnetic spacer.[5] In both cases much attention has been paid on the study of the rigidity[6] and the thermal stability[7] of the hard layer. However, other effects related to the interaction between the hard and the soft layer, such as domain wall duplication effects, have not been considered for the spin valves, contrary to magnetic tunnel junctions.[8,9]

In this paper, we report on the interaction between a soft Fe/Co bilayer and an antiferromagnetic CoFe/Ir/CoFe sandwich, in molecular-beam epitaxy (MBE) grown hard-soft spin-valve-type structures with the following nomenclature: $MgO(001)//Fe_{5\ nm}/Co_{0.5\ nm}/Cu_{3\ nm}/Co_{0.5\ nm}/[CoFe_{1.5\ nm}/Ir_{0.5\ nm}/CoFe_{3\ nm}]/Cu_{2\ nm}/Cr_{2\ nm}$. First, the magnetization and the magnetoresistance loops of the whole stack show a well-defined plateau in a large field window, which is interesting for applications. Second, it is clearly shown that the magnetization minor loop corresponding to the switch of the soft layer is shifted by 5 Oe in comparison with the loop measured for the sample containing only the soft layer. This is induced by an exchange-type interaction between the soft and the hard layer. The exchange interaction is also responsible for a magnetic structure duplication from the hard into the soft magnetic electrode. This duplication is evidenced by the gaint magnetoresistance (GMR) measurements which are very sensitive to investigate local magnetization variations, and supported by magnetic force microscopy (MFM) and demagnetization studies.

II. SAMPLE PREPARATION

$CoFe_{1.5\ nm}/Ir_{0.5\ nm}/CoFe_{3\ nm}$ sandwiches have been deposited by MBE on MgO(001) substrates covered with a Fe/Co/Cu/Co buffer,[10] in which the Fe/Co constitutes a soft magnetic subsystem of the spin valve. Within the sandwich, the CoFe films correspond to an alloy with 50 at. % Co and 50 at. % Fe, and the Ir thickness (0.5 nm) corresponds to the first AF maximum of the coupling strength,[11–13] providing a value that exceeds -3.5 erg/cm^2. The substrates were heated at 600 °C for 1 h prior to deposition, then cooled to room temperature (rt). The base pressure was about 1×10^{-10} mbars, and the deposition rates were typically about 0.3 nm/min. Fe was deposited at 500 °C in order to obtain a flat surface and a monocrystalline layer. The rest of the stack was deposited at rt in order to avoid diffusion at interfaces. The growth quality was monitored using an *in situ* reflection high-energy electron diffraction (RHEED) technique. The RHEED patterns showed a good monocrystalline quality with a bcc structure for the Fe layer. This is at the origin of a fourth degree magnetic anisotropy for the Fe layer with the magnetization easy axis along the [100] Fe direction.[14] In order to study separately the magnetization reversal of the Fe layer, an additional sample consisting of a soft Fe/Co/Cu buffer has been grown with Fe deposited at 500 °C and capped with an $Ir_{2\ nm}$ protection layer.

III. RESULTS AND DISCUSSION

A. Magnetization and magnetoresistance major loops

Figure 1 presents the magnetization and magnetoresistance major loops for the $MgO(001)//Fe_{5\ nm}/Co_{0.5\ nm}/$

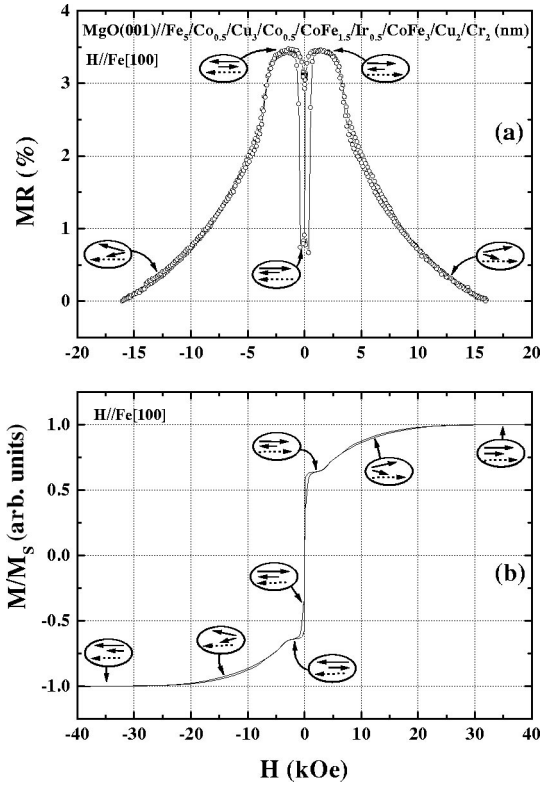

FIG. 1. Room-temperature magnetoresistance (a) and magnetization (b) major loops for the $MgO(001)//Fe_{5\ nm}/Co_{0.5\ nm}/Cu_{3\ nm}/Co_{0.5\ nm}/[CoFe_{1.5\ nm}/Ir_{0.5nm}/CoFe_{3\ nm}]/Cu_{2\ nm}/Cr_{2nm}$ spin valve, with the magnetic field applied in the film plane and along the [100] Fe direction. Going from the positive saturation, the arrows show the successive magnetic configurations. The dotted arrow corresponds to the soft detection layer. The small and the large solid arrows correspond to the magnetic moments of the bottom and the top CoFe layer of the AAF, respectively.

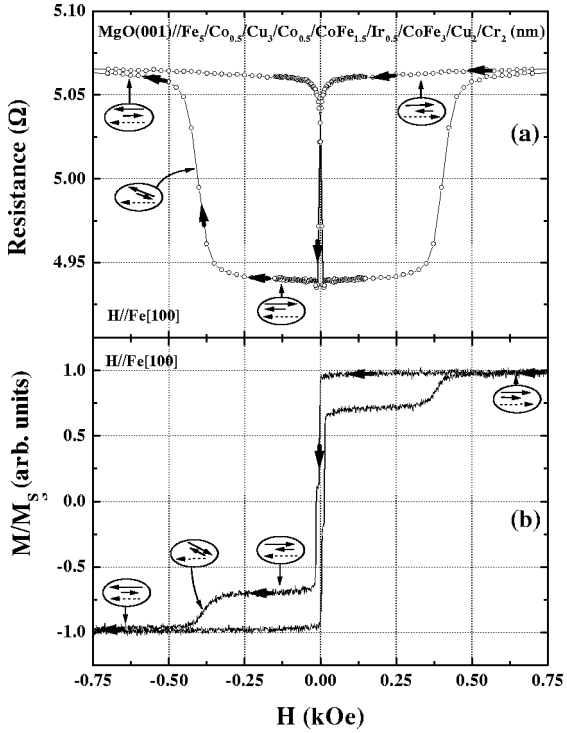

FIG. 2. Zoom of the magnetoresistance (a) and magnetization (b) major loops reported in Fig. 1 for the $MgO(001)//Fe_{5\ nm}/Co_{0.5\ nm}/Cu_{3\ nm}/Co_{0.5\ nm}/[CoFe_{1.5\ nm}/Ir_{0.5\ nm}/CoFe_{3nm}]/Cu_{2\ nm}/Cr_{2\ nm}$ spin valve. The magnetic field was applied in the film plane and along the [100] Fe direction. Arrows are reported to show the successive magnetic configurations. The dotted arrow corresponds to the soft detection layer. The small and the large solid arrows correspond to the magnetic moments of the bottom and the top CoFe layer of the AAF, respectively.

$Cu_{3\ nm}/Co_{0.5\ nm}/[CoFe_{1.5\ nm}/Ir_{0.5\ nm}/CoFe_{3\ nm}]/Cu_{2\ nm}/Cr_{2\ nm}$ spin valve measured at room temperature with the magnetic field in the plane and parallel to the magnetization easy axis, i.e., Fe [100]. These curves show a strong antiferromagnetic coupling between the CoFe layers of the AAF, of the order of -3.5 erg/cm^2. The quality of the coupling is certified by: (i) a plateau up to -3 kOe, where the CoFe magnetization vectors have an antiparallel alignment, and (ii) a variation of the magnetization and magnetoresistance curves between the plateau and the saturation fields, close to the one expected of a perfect antiferromagnetic coupling. In order to have more insight on the reversal mechanisms of the soft and the hard electrode, we have zoomed the magnetization and magnetoresistance major loops as reported in Fig. 2. After the field reversal, the switch of the Fe/Co soft bilayer occurs at $H_{C1}=-15$ Oe, giving rise to the most interesting situation where the Fe/Co magnetization is antiparallel to the net magnetization of the AAF. Such an alignment is stable until the coercive field of the AAF $H_{C2}=-400$ Oe, where an abrupt switch of the AAF net moment is observed leading to a sharp increase in the resistance. Therefore, the magnetization vector of the AAF's thinnest layer is again antiparallel to the magnetization vector of the soft bilayer. This configuration is preserved until a field of -3 kOe, where the field strength is high enough to overcome the antiferromagnetic interaction. Consequently, the moments of the thick and thin CoFe layers start to rotate, respectively, clockwise and anticlockwise to follow the applied field direction.

Compared to the most commonly used Ru-based AAF,[6] the Ir-based AAF presents more interesting characteristics. This is mainly due to the deposition technique. A good rigidity is not only defined by a large coercive field, but also by a sharp reversal of the net magnetic moment of the AAF. In the present case, this is easily visible on the magnetization and magnetoresistance loops which present a well-defined plateau between the coercive fields H_{C1} and $H_{C2}=400$ Oe of the soft and the hard layers. This field interval that defines the operating field window of a spin-valve system, as well as the stability of the AAF, is essential for magnetic sensor applications. On the contrary, in the case of Ru-based AAF's (generally prepared by magnetron sputtering) and within the field window, the net moment of the AAF rotates progressively by increasing the field and the hard layer is far to present a good stability. To our knowledge, Ru-based AAF's has never presented a similar rigidity to the one evidenced in the present case, but we have to keep in mind that our samples were prepared under more special conditions.

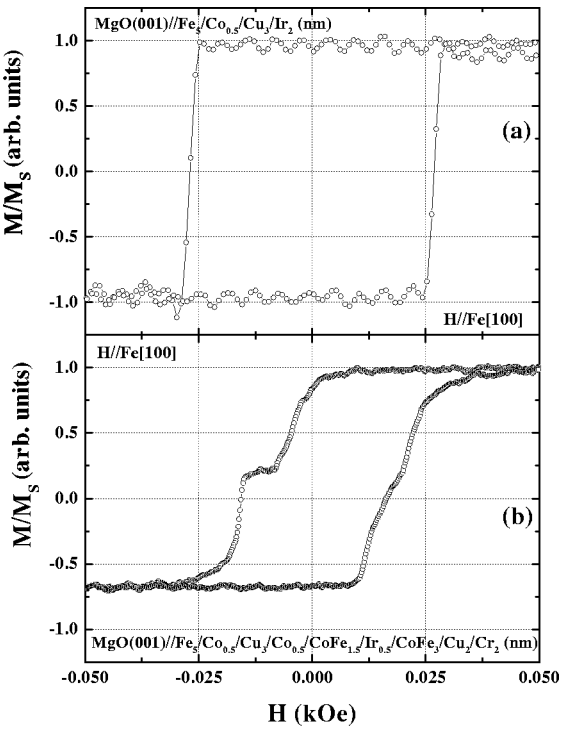

FIG. 3. Magnetization loops for (a) the MgO(001)// $Fe_{5\ nm}/Co_{0.5\ nm}/Cu_{3\ nm}/Ir_{2\ nm}$ buffer stack and (b) for the MgO(001)// $Fe_{5\ nm}/Co_{0.5\ nm}/Cu_{3\ nm}/Co_{0.5\ nm}/[CoFe_{1.5\ nm}/Ir_{0.5\ nm}/CoFe_{3\ nm}]/Cu_{2\ nm}/Cr_{2\ nm}$ spin valve. Measurements have been performed at room temperature with an in-plane magnetic field and along the [100] Fe direction.

B. Exchange-type interaction between the hard and the soft layers

In order to have more details on the reversal mechanism of the soft subsystem, we have to look carefully to its reversal before and after the deposition of the AAF. This soft bilayer should present a small coercive field in order to follow freely any magnetic applied field, and a sharp reversal when the field is switched. This is exactly what is observed in Fig. 3(a) that shows the magnetization loop at room temperature for the Fe when only the buffer layer is deposited. The magnetic field is applied along the Fe [100] direction, which means the magnetization easy axis. The loop is square with a coercive field of about 25 Oe. This coercive field is reduced to 18 Oe after the growth of the AAF sandwich [Fig. 3(b)]. More interestingly, the loop is asymmetric and is shifted towards positive field values by about 5 Oe. This can be attributed to a ferromagnetic-type interaction between the Fe soft layer and the AAF. Indeed, coming from positive field values the magnetization is constant. After the field reversal, a switch of 50% of the magnetization of the Fe layer is first observed, followed by a plateau. This is due to the fourth-order magnetic anisotropy of the Fe layer, which reaches an easy axis after a $\pm 90°$ rotation. Therefore, the complete rotation is observed when the external field overcomes the magnetic anisotropy. The situation is, however, different when coming from negative field values. Due to the ferromagnetic interaction the loop is shifted and the plateau is no more observed. This is explained by the fact that the magnetization rotation occurs at a magnetic field higher than the magnetic anisotropy strength. As a consequence of the ferromagnetic interaction, a domain wall structure may be duplicated from the thinnest CoFe layer into the Fe/Co soft bilayer, despite the 3 nm thickness of the decoupling Cu layer.

It is important to note that different types of interactions between the hard and the soft electrode can be at the origin of such behavior. These interactions may have several origins such as exchange-type interaction, dipolar interaction, or orange-peel interaction. The dipolar interaction is generated by the stray field of both magnetic layers of the AAF on the Fe/Co detection bilayer. This interaction is thus related to the magnetic inhomogeneities of the AAF and is dependent on both the thickness of the CoFe layers and on their distance d from the Fe layer as $1/d^2$ (when d is about the same order of magnitude as the layer thickness). In these conditions and using a simple calculation, it is clear that the stray field coming from the thin CoFe layer is stronger than the one coming from the upper thick CoFe layer. This stray field will then favor an antiferromagnetic interaction between the thin CoFe layer and the Fe detection layer. This is in contradiction with the ferromagnetic-type interaction already evidenced by the minor magnetization loop, but does not exclude the possibility of the existence of this type of interaction. However, since the magnetization minor loop is shifted towards positive fields, the antiferromagnetic interaction is overcomed by the exchange (ferromagnetic) interaction. On the other hand, an orange-peel-type interaction across the Cu decoupling layer is limited since, as atomic force microscopy observations indicated, the roughness of the free surfaces adjacent to this layer are characterized by very small peak-to-peak values which never exceed 0.5 nm, compared with the thickness of the Cu layer (3 nm). Therefore, the most probable explanation seems to be an exchange-type interaction between the Fe/Co electrode and the thin CoFe layer of the AAF.

C. Magnetoresistance minor loop and magnetic configuration

To further support the existence of this interaction and to confirm the biasing effect of the Fe soft layer, magnetoresistance minor loops have been recorded and presented in Fig. 4. In order to make the understanding of this curve easier for the reader, a schematic explanation of the successive domain configurations in the magnetic layers for different fields is given in Fig. 5.

First, we will explain using physical arguments the magnetic configuration shown in Fig. 5(a). Decreasing the field from positive saturation, the local magnetic moments of the thin CoFe layer start to rotate driven by the AF coupling. The moments will rotate clockwise and anticlockwise depending on their local anisotropy axes with respect to the field direction. The regions where the local anisotropy axis is in the field direction will constitute the core of the future walls, if the magnetization of adjacent regions relax by rotating in the opposite directions. Therefore, by reducing the field, the magnetization of such adjacent regions will turn by 180°, giving rise to 360° Néel domain walls. These walls are par-

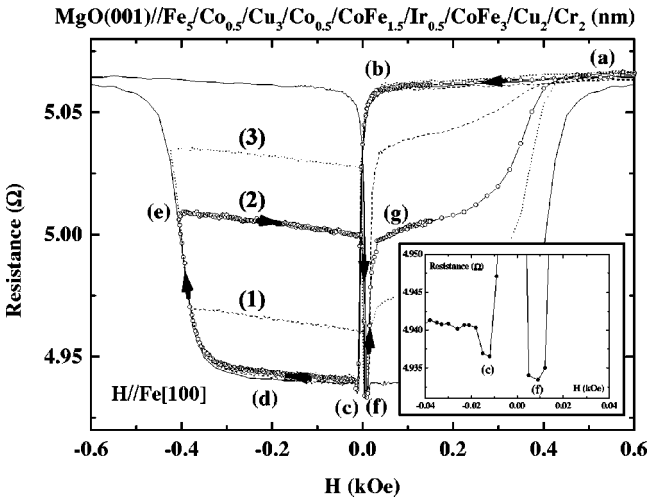

FIG. 4. Magnetoresistance minor loops measured at room temperature with an in-plane magnetic field for MgO(001)// $Fe_{5\ nm}$ / $Co_{0.5\ nm}$ / $Cu_{3\ nm}$ / $Co_{0.5\ nm}$ / [$CoFe_{1.5\ nm}$ /$Ir_{0.5\ nm}$ /$CoFe_{3\ nm}$]/ $Cu_{2\ nm}$ /$Cr_{2\ nm}$ spin valve. Solid line corresponds to the zoomed loop reported in Fig. 2(a). Open circles correspond to an incomplete minor loop from 750 Oe to −375 Oe and again to 750 Oe. The letters indicate different resistance states corresponding to the magnetic configurations reported in Fig. 5. The inset presents a zoom of the GMR minor loop (curve 2) around zero field.

ticularly stable since their core magnetization is aligned in the field direction [thin bottom CoFe layer in Fig. 5(a)]. For fields smaller than the plateau field H_P (~3 kOe), and due to the strong AF coupling, this domain structure will be duplicated into the upper (thick) CoFe layer. In this layer, the magnetic walls will present the core magnetization in the opposite field direction. The existence of these 360° domain walls will be experimentally evidenced later. Therefore, in the plateau, corresponding to a high resistance state indicated by *a* in Fig. 4, the magnetizations of the CoFe layers are antiparallel with a domain structure as shown in the Fig. 5(a). The Fe/Co bilayer has its magnetization antiparallel to the nearest CoFe layer and is perfectly aligned in the field direction. With decreasing the applied field, this state is preserved until 50 Oe. Below this value, the alignment of the CoFe moments of the two layers is still antiparallel, but the local net moment turns towards the local anisotropy axis (zone *b* in Fig. 4). This leads to a reduction of the magnetization of the CoFe layers along the field direction, and thus to a reduction of the GMR signal coming from the soft electrode. After the field reversal, from the zone *b* to the zone *c* in Fig. 4, a sharp decrease in the resistance is observed. The magnetizations of some regions of the Fe layer are switching clockwise, while other regions exhibit an anticlockwise rotation, leading to a domain structure. Such a domain structure is a duplication of one of the thin CoFe layers as a result of the exchange-type interaction. Thus, in the zone *c* of Fig. 4, a complete parallel alignment of the magnetizations from both the domains and the walls is reached between the Fe and the thin CoFe layers. In these conditions, the lowest resistance state is obtained. Upon decreasing the field, the resistance increases and becomes constant around −15 Oe

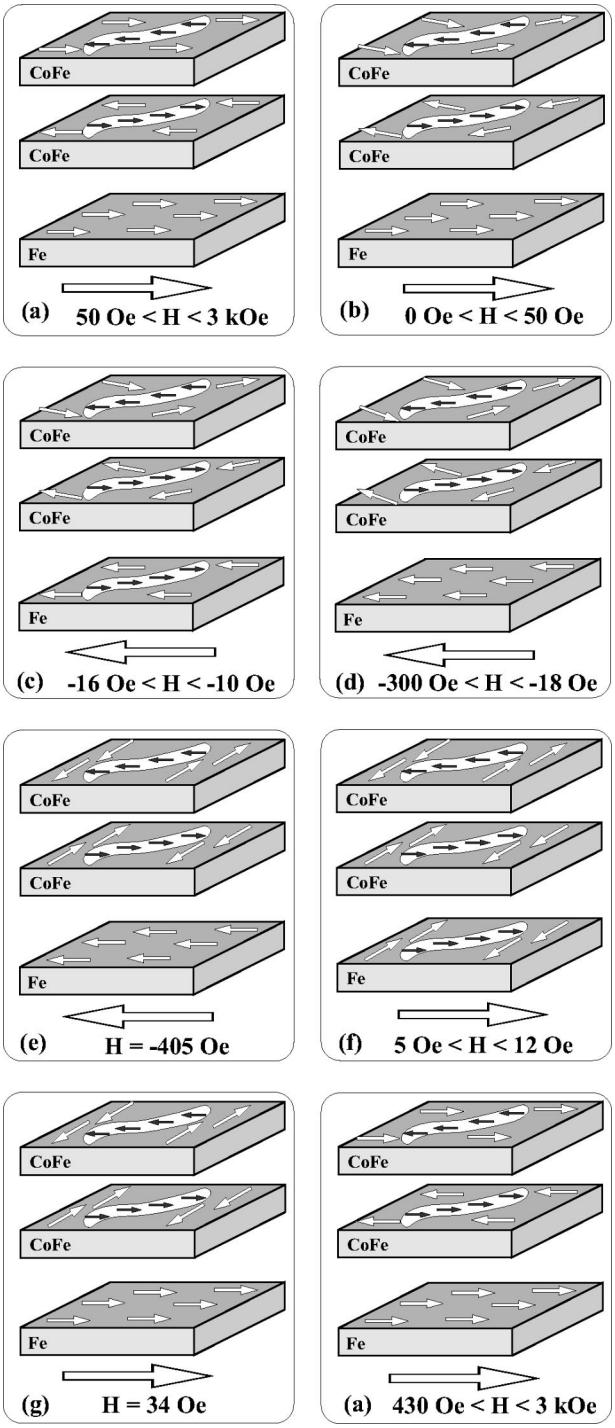

FIG. 5. Successive magnetic configurations corresponding to the resistance states indicated in Fig. 4. For each magnetic layer white arrows represent the local magnetization in each domain. In addition, the narrow white band with small dark arrows represents a domain wall with the core magnetic moments. The big white arrow corresponds to the direction of the external field and the values indicate the field range that corresponds to the magnetic configuration.

as shown in zone *d* of Fig. 4. This means that the applied field is high enough to overcome the ferromagnetic interaction and to annihilate the domain wall structure from the detection layer [Fig. 5(d)].

In order to further support the explanation given above, we have performed an additional irreversible minor loop inside the GMR loop described above. This means that by decreasing the negative applied field, we have stopped the field before the complete reversal of the AAF, exactly at the middle of the resistance slope in the zone *e* of the magnetoresistance loop (Fig. 4, curve 2). The magnetic configuration of this intermediate resistance state is shown in Fig. 5(e), where the antiferromagnetic sandwich has rotated by only 90° with respect to the applied field and to the magnetization vector of the soft bilayer. With increasing the magnetic field towards zero, the resistance shows a very small slope which is due to a slight disorientation of the applied field with respect to the easy axis. After the field reversal, the resistance drops to reach its lowest value around 5 Oe, zone *f* in Fig. 4. In this state the antiparallel alignment in the AAF is perfect, and both the magnetic net moment of the AAF and the magnetization of the soft electrode are perpendicular to the external field. This means that the magnetization of the Fe/Co bilayer rotates by only $\pm 90°$ to be completely parallel to the nearest CoFe layer and to give rise to the low resistance state, as shown in Fig. 5(f). This is possible due the fourth-order magnetic anisotropy of the Fe layer and/or due to the ferromagnetic interaction between the Fe and the thin CoFe layers. In order to see which one of these two contributions is the most important, we also analyzed GMR minor loops where the angle between the magnetic net moment of the AAF and the field after the field reversal [analogous to the zone *e* in Fig. 4], is more (curve 3) or less (curve 1) than 90°. This means that the angle between the thin CoFe layer and the field direction (Fe/Co magnetization) is different from 90°. In these conditions, if the Fe/Co magnetization will still switch by $\pm 90°$ towards easy magnetization axis, when the field is reversed towards positive values, the resistance will not reach its lowest state, since the local moments of the Fe/Co and thin CoFe layer will not be perfectly parallel. Nevertheless, this low resistance state is systematically reached no matter how much the AAF net moment is rotated with respect to the field axis. This indicates that the ferromagnetic interaction is stronger than the one due to the anisotropy of the Fe layer. Therefore, the magnetic structure of the thin CoFe layer is fully duplicated into the Fe/Co bilayer (zone *f* in Fig. 4). Such a domain configuration is frozen in a small field window where the ferromagnetic interaction is high enough with respect to the external field strength. For larger external field, the resistance increases, zone *g* in Fig. 4, to reach, in the case of curve 2, its previous value before the Fe/Co switching. This means that the domain wall structure is annihilated and the rotation of the Fe/Co magnetization is then complete and is lying in the external field direction as shown in Fig. 5(g). Upon further increasing the magnetic field, the AAF rotates before the coercive field is reached and aligns its magnetic net moment in the field direction. This is due to the initial configuration of the AAF net moment, which is perpendicular to the external field in comparison with the antiparallel alignment in the normal situation.

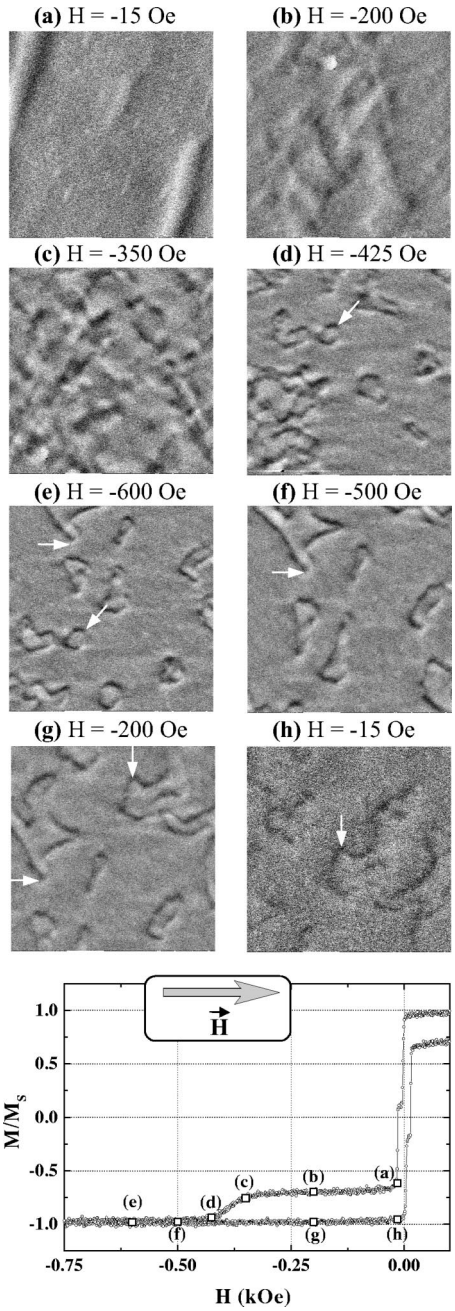

FIG. 6. Set of MFM images (10×10 μm^2) for the [Fe/Co]/Cu/[Co/CoFe/Ir/CoFe] structure, showing the magnetization reversal and the existence of a domain structure at some significant magnetic-field values, indicated in the magnetization curve. The detection layer gives no contrast since it is completely saturated. White arrows indicate stable Néel walls.

D. Magnetic force microscopy observations

This simple model of magnetization reversal describes well the magnetic configuration of the sample in Fig. 5, in agreement with the minor GMR loops, and is realistic since domain walls were evidenced by MFM observations. Indeed, Fig. 6 shows that decreasing the field from zero to -15 Oe, the contrast is small, and large magnetized regions are observed. Therefore, the dipolar interaction generated by the stray field and predicted by Thomas *et al.*[9] is small, and

the ferromagnetic-type interaction prevails. The magnetic contrast arises solely from the hard layer since the soft detection layer is saturated, and increases progressively with the external field as the net moment of the AAF starts to deviate from the field axis.[15] After the complete reversal of the net magnetic moment of the AAF ($^{-}$400 Oe), 360° domain walls are observed. It is important to note that these walls are stable in the plateau after the AAF switch, as well as when the field is reduced down to $^{-}$15 Oe. In this last case, the walls appear with small contrast since the magnetization corresponding to adjacent domains relax towards local anisotropy axes, thus reducing the angle of the walls. Therefore, for small fields, a domain structure exists in the hard layer and is duplicated into the soft magnetic electrode as it was shown by the transport measurements.

E. Demagnetization studies

The interaction between the hard and the soft magnetic electrodes can be also evidenced by repeated switches of the soft layer magnetization. This type of measurements can give an indication on the stability of the AAF system, which is required for the applications, i.e. on the evolution of the magnetic domain structure in this electrode. If such evolution exists, it will be reflected on the rigidity of the hard layer and consequently on the reversal mechanism of the soft layer, thus confirming the interaction between the soft and the hard layers. Therefore, 10^4 cycles with a maximum applied field of 100 Oe have been performed in order to obtain repeated magnetization reversals of the soft layer. This field saturates completely the soft layer, but should not influence the hard AAF system (as observed in Fig. 2). Therefore, a magnetization major loop recorded after the repeated switches should be identical to the one measured previous to the cycling experiment. Nevertheless, the magnetization major and minor loops [Figs. 7(a) and 7(b)] measured after the repeated switches of the Fe/Co soft bilayer are significantly different from the loops reported in Figs. 2(b) and 3(b). These differences are a strong indication of significant changes in the AAF system.

First, one observes that the rigidity of the AAF hard layer is reduced after performing the repeated switches. Indeed, after the reversal of the soft layer, the plateau corresponding to the situation where the net moment of the AAF is opposite to the field direction is not well defined [like in Fig. 2(b)], but a slope is observed indicating a continuous rotation of the AAF magnetization [Fig. 7(a)]. Moreover, for fields higher than 400 Oe, a long tail of magnetization is observed up to the complete alignment of the AAF's net magnetic moment towards the direction of the applied field. This means that the AAF's rigidity is reduced, indicating clearly the presence of a domain structure in the AAF. This is induced by cycling experiment and is the result of the interaction between the hard and the soft magnetic electrodes of the spin valve. Moreover, after the repeated switches of the soft magnetic layer, the shape of the minor magnetization loop [Fig. 7(b)] is also modified. The magnetization of the Fe/Co bilayer switches in a continuous rotationlike manner characterized by a small remnant magnetization and coercive field. However, the bias field is still positive and of the same value (5 Oe) as in the case of the minor loop measured before cycling [Fig. 3(b)], which indicates that in the both cases the average interaction between the soft and the hard electrodes of the spin valve is unchanged. These observations indicate that a domain structure is present in the AAF system around zero field as it was already confirmed by the MFM studies.

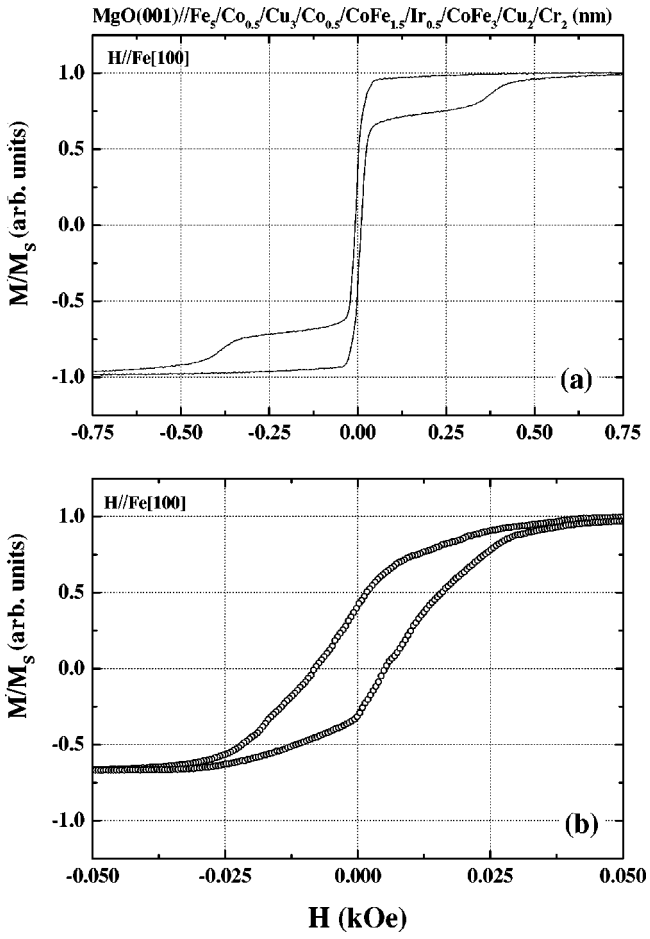

FIG. 7. Major (a) and minor (b) magnetization loops measured after 2×10^4 reversals of the Fe/Co magnetization. During the cycling experiment and the magnetic measurement, the magnetic field was applied in the film plane along the [100] Fe direction.

IV. CONCLUSIONS

In conclusion, we succeeded to obtain high-quality spin valves using a CoFe/Ir/CoFe AAF system as a hard magnetic electrode. This AAF presents a very good rigidity in terms of coercive field and stability in the external field. The most interesting result was obtained by using the magnetoresistive effect as a sensitive probe for micromagnetic characterization. By analyzing the magnetoresistive signal of the spin valves, we evidenced a duplication of the magnetic domain structure from the hard into the soft magnetic electrode, due to a predominant exchange-type interaction. It is clearly shown that this phenomenon appears despite the large thick-

ness of the decoupling layer (3 nm), and is supported by MFM observations and demagnetization studies. The repeated reversals of the soft layer modify the magnetic domain structure of the hard electrode and lead to a degradation of its rigidity. This magnetic domain structure is mirrored in the reversal behavior of the soft layer magnetization and is consistent with the domain wall duplication evidenced by transport measurements. To our knowledge, such duplication was never reported for spin-valve systems containing only metallic layers.

ACKNOWLEDGMENTS

Authors thanks J. Arabski and G. Schmerber for sample preparation, and M. Guth for GMR measurements. This work was supported by the European Community ''TunelSense'' project (Grant No. BRPR-CT98-0657).

*Email address: aziz.dinia@ipcms.u-strasbg.fr

[1] B. Dieny, V.S. Speriosu, S.S.P. Parkin, B.A. Gurney, D.R. Wilhoit, and D. Mauri, Phys. Rev. B **43**, 1297 (1991); R. Kergoat, J. Miltat, T. Valet, and R. Jrome, J. Appl. Phys. **76**, 7087 (1994).

[2] V.S. Speriosu, J.P. Nozieres, B.A. Gurney, B. Dieny, T.C. Huang, and H. Lefakis, Phys. Rev. B **47**, 11 579 (1993); C. Mény, J.P. Jay, P. Panissod, P. Humbert, V.S. Speriosu, H. Lefakis, J.P. Nozieres, and B.A. Gurney, in *Magnetic Ultra Thin films, Multilayers and Surfaces/Interfaces and Characterization*, edited by B.T. Jonker, S.A. Chambers, R.F.C. Farrow, C. Chappert, R. Clarke, W.J.M. de Jorge, T. Egani, P. Grünber, K.M. Krishnan, E.E. Marinero, C. Rau, and S. Isunashima, Mater. Res. Soc. Symp. Proc. MRS Symposia Proceedings No. **313** (Material Research Society, Pittsburg, 1993), p. 289; P. Panissod, J.P. Jay, C. Mény, M. Wójcik, and E. Jedryka, Hyperfine Interact. **97/98**, 75 (1996).

[3] H.J.M. Swagten, G.J. Strijkers, P.J.H. Bloemen, M.M.H. Willekens, and W.J.M. de Jonge, Phys. Rev. B **53**, 9108 (1996); W.F. Egelhoff, Jr., P.J. Chen, C.J. Powell, M.D. Stiles, J.H. Hudy, K. Takano, and A.E. Berkowitz, J. Appl. Phys. **82**, 6142 (1997).

[4] H.N. Fuke, K. Saito, Y. Kamaguchi, H. Iwasaka, and M. Sahashi, J. Appl. Phys. **81**, 4004 (1997).

[5] H.A.M. van den Berg, W. Clemens, G. Gieres, G. Rupp, M. Vieth, J. Wecker, and S. Zoll, J. Magn. Magn. Mater. **165**, 524 (1997).

[6] C. Tiusan, T. Dimopoulos, M. Hehn, V. Da Costa, Y. Henry, H.A.M. van den Berg, and K. Ounadjela, Phys. Rev. B **61**, 580 (2000).

[7] T. Dimopoulos, C. Tiusan, V. Da Costa, K. Ounadjela, and H.A.M. van den Berg, Appl. Phys. Lett. **77**, 3624 (2000).

[8] M. Hehn, O. Lenoble, D. Lacour, C. Fery, M. Piecuch, C. Tiusan, and K. Ounadjela, Phys. Rev. B **61**, 11 643 (2000); M. Hehn, O. Lenoble, D. Lacour, and A. Schuhl, *ibid.* **62**, 11 344 (2000); O. Lenoble, M. Hehn, D. Lacour, A. Schuhl, D. Hrabovsky, J.F. Bobo, B. Diouf, and A.R. Fert, *ibid.* **63**, 052409 (2001).

[9] L. Thomas, J. Lüning, A. Scholl, F. Nolting, S. Anders, J. Stöhr, and S.S.P. Parkin, Phys. Rev. Lett. **84**, 3462 (2000); L. Thomas, M.G. Samant, and S.S.P. Parkin, *ibid.* **84**, 1816 (2000).

[10] S. Colis, A. Dinia, D. Deck, G. Schmerber, and V. Da Costa, J. Appl. Phys. **88**, 1552 (2000).

[11] A. Dinia, M. Stoeffel, K. Rahmouni, D. Stoeffler, and H.A.M. van den Berg, Europhys. Lett. **42**, 331 (1998).

[12] S. Colis, A. Dinia, C. Mény, P. Panissod, C. Ulhaq-Bouillet, and G. Schmerber, Phys. Rev. B **62**, 11 709 (2000).

[13] Y. Luo, M. Moske, and K. Samwer, Europhys. Lett. **42**, 565 (1998); Y. Luo, B. Pfeifer, A. Kaeufler, M. Moske, and K. Samwer, J. Appl. Phys. **87**, 2479 (2000).

[14] S. Colis and A. Dinia, J. Appl. Phys. **91**, 5268 (2002).

[15] The reversal of the magnetic moments follows basically a rotational process [C. Tiusan, T. Dimopoulos, K. Ounadjela, and M. Hehn, Phys. Rev. B **64**, 104423 (2001)], and not a nucleation/propagation process [N. Persat, H.A.M. van den Berg, and A. Dinia, *ibid.* **62**, 3917 (2000)]. In our case the walls are stable, and they are not propagating when increasing the applied field.